articles

molecular pharmaceutics

Improved Efficacy of $\alpha_v\beta_3$-Targeted Albumin Conjugates by Conjugation of a Novel Auristatin Derivative

Kai Temming,*,†,‡ Damon L. Meyer,§ Roger Zabinski,§ Peter D. Senter,*,§ Klaas Poelstra,† Grietje Molema,|| and Robbert J. Kok†,⊥

Department of Pharmacokinetics and Drug Delivery, University Center for Pharmacy, University of Groningen, Groningen, The Netherlands, Seattle Genetics, Bothell, Washington , KREATECH Biotechnology B.V., Amsterdam, The Netherlands, Medical Biology Section, Department of Pathology and Laboratory Medicine, University Medical Center Groningen, University of Groningen, Groningen, The Netherlands, and Department of Pharmaceutics, Utrecht Institute for Pharmaceutical Sciences, Utrecht University, Utrecht, The Netherlands

Received March 21, 2007; Revised Manuscript Received June 12, 2007; Accepted June 19, 2007

Abstract: Cellular handling of drug delivery preparations en route to the lysosomal compartment has been extensively studied, but little is known about cellular handling of drugs subsequent to their release from the delivery system. We studied a series of closely related drug targeting conjugates, consisting of albumins equipped with $\alpha_v\beta_3$-selective RGD-peptide homing ligands, PEG stealth domains, and either the antitubulin agent monomethyl auristatin E (MMAE) or a new F-variant (MMAF). Since MMAF has a C-terminal charge, this compound is potentially less prone to passive redistribution after its release from the carrier. We demonstrate that RGD-peptide-equipped albumin conjugates with MMAF were indeed more potent than MMAE conjugates, in killing both $\alpha_v\beta_3$-positive tumor cells and proliferating endothelial cells. Efficacy increased more in tumor cells than in endothelial cells, suggesting different drug redistribution behavior for the two cell types. Binding affinity and uptake of the conjugate *and* the cellular handling of released drug contributed to the final efficacy of drug–carrier conjugates, highlighting the importance of all aspects to be carefully considered in the design of targeted drug delivery preparations.

Keywords: RGD; redistribution; prodrug; targeting; drug targeting; apoptosis; endothelial cells; antivascular therapy; angiogenesis

Introduction

The formation of new blood vessels through angiogenesis is an essential step in the growth of solid tumors and facilitates the supply of oxygen and nutrients to the tumor mass. In later stages of cancer, continuous remodeling of the intratumoral vascular bed allows spreading of metastatic tumor cells to other tissues. In the early 1970s, J. Folkman proposed antiangiogenic or antivascular therapy for the treatment of cancer, and vascular-directed therapies are currently under extensive investigation.[1,2] One way to destroy tumor vessels consists of the induction of apoptosis in vascular endothelium and pericytes. However, most cytotoxic compounds are selective neither for endothelial cells and pericytes in general nor for angiogenic endothelium and pericytes. Consequently, their applicability is limited due to

* To whom correspondence should be addressed: Department of Pharmacokinetics and Drug Delivery, Antonius Deusinglaan 1, 9813 AV Groningen, The Netherlands. Telephone: +31 50 363 7627. Fax: +31 50 363 3247. E-mail: k.temming@rug.nl.

† University Center for Pharmacy, University of Groningen.

‡ KREATECH Biotechnology B.V.

§ Seattle Genetics.

|| University Medical Center Groningen, University of Groningen.

⊥ Utrecht University.

(1) Folkman, J.; Merler, E.; Abernathy, C.; Williams, G. Isolation of a tumor factor responsible for angiogenesis. *J. Exp. Med.* **1971**, *133*, 275–288.

(2) Ferrara, N.; Kerbel, R. S. Angiogenesis as a therapeutic target. *Nature* **2005**, *438*, 967–974.

10.1021/mp0700312 CCC: $37.00
Published on Web 08/08/2007

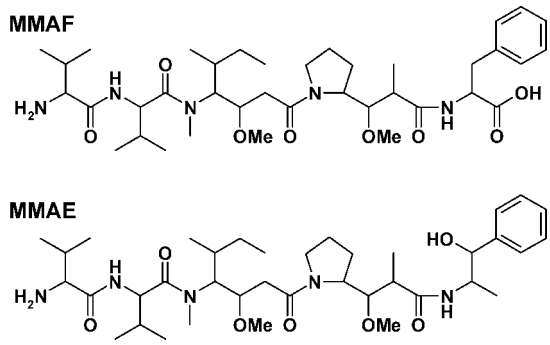

Figure 1. Chemical structures of monomethyl auristatin E (MMAE) and F (MMAF).

systemic toxicity. To create proapoptotic or antiangiogenic therapies that can specifically induce apoptosis in angiogenic endothelial cells, we recently developed RGD-equipped monomethyl auristatin E (MMAE)–albumin conjugates.[3] Similarly, we developed drug delivery conjugates that inhibited angiogenesis by selectively intervening in VEGF signaling.[4] Cell selectivity in these approaches was gained by coupling of cyclic RGD-peptides with high affinity for $\alpha_v\beta_3$-integrin to the albumin carrier. We furthermore prepared multivalent RGD–albumin conjugates as such multivalent ligands are known to be internalized in contrast to single RGD-peptide constructs.[5] Apart from albumin as a carrier, RGD-equipped HPMA copolymers have also been used successfully for the delivery of drug to tumor blood vessels.[6,7] The RGD-peptides represent a ligand that binds to $\alpha_v\beta_3$-integrin.[8] The $\alpha_v\beta_3$-integrin target receptor is overexpressed on angiogenic endothelium, and its expression is minimal on quiescent endothelial cells and highly limited to selective reticuloendothelial cells in other healthy tissue.[9,10] The restricted expression profile and the good accessibility of endothelial cells make them an ideal target receptor for cell-specific therapies.[11] As a consequence, RGD-driven delivery of therapeutics and imaging agents has become a popular technology, in parallel to antibody-driven targeting strategies.[12,13]

Redistribution of targeted drugs is a major limitation of drug targeting approaches. Although the initial binding and subsequent internalization of targeted therapeutics are often well studied, further processing of the therapeutic and cellular handling of the released compound are ill understood.[14–16] Both metabolism and drug efflux can terminate the pharmacological activity of the drug. Especially in endothelial cells that are in constant contact with the bloodstream, conveyance of the compound in the circulation will drive a rapid, diffusion-controlled efflux of the drug from the intracellular environment. We now report on the development of RGD-equipped drug–albumin conjugates with the drug monomethyl auristatin F (MMAF, Figure 1), which was designed in part to circumvent such redistribution pathways and was therefore expected to accumulate to a higher extent in target cells.[17] MMAF contains a C-terminal domain that is charged at physiological pH, thereby impairing passive redistribution (Figure 1).[17]

The closely related auristatins MMAE and MMAF were conjugated to RGD-equipped albumin carriers, which are classified as biocompatible and biodegradable polymeric carriers. These drug targeting conjugates were evaluated for drug and RGD-peptide content, and the influence of PEGylation on hydrodynamic volume was determined. We studied

(3) Temming, K.; Meyer, D. L.; Zabinski, R. F.; Dijkers, E. C. F.; Poelstra, K.; Molema, G.; Kok, R. J. Evaluation of RGD-targeted Albumin Carriers for Specific Delivery of Auristatin E to Tumor Blood Vessels. *Bioconjugate Chem.* **2006**, *17*, 1385–1394.
(4) Temming, K.; Lacombe, M.; Schaapveld, R. Q. J.; Orfi, L.; Keri, G.; Poelstra, K.; Molema, G.; Kok, R. J. Rational Design of RGD-albumin conjugates for targeted delivery of the VEGF-R kinase inhibitor PTK787 to angiogenic endothelium. *ChemMedChem* **2006**, *11*, 1200–1203.
(5) Boturyn, D.; Coll, J. L.; Garanger, E.; Favrot, M. C.; Dumy, P. Template assembled cyclopeptides as multimeric system for integrin targeting and endocytosis. *J. Am. Chem. Soc.* **2004**, *126*, 5730–5739.
(6) Mitra, A.; Mulholland, J.; Nan, A.; McNeill, E.; Ghandehari, H.; Line, B. R. Targeting tumor angiogenic vasculature using polymer-RGD conjugates. *J. Controlled Release* **2005**, *102*, 191–201.
(7) Mitra, A.; Coleman, T.; Borgman, M.; Nan, A.; Ghandehari, H.; Line, B. R. Polymeric conjugates of mono- and bi-cyclic αVβ3 binding peptides for tumor targeting. *J. Controlled Release* **2006**, *114*, 175–183.
(8) Pierschbacher, M. D.; Ruoslahti, E. Cell attachment activity of fibronectin can be duplicated by small synthetic fragments of the molecule. *Nature* **1984**, *309*, 30–33.
(9) Hood, J. D.; Cheresh, D. A. Role of integrins in cell invasion and migration. *Nat. Rev. Cancer* **2002**, *2*, 91–100.
(10) Jin, H.; Varner, J. Integrins: Roles in cancer development and as treatment targets. *Br. J. Cancer* **2004**, *90*, 561–565.
(11) Schraa, A. J.; Everts, M.; Kok, R. J.; Asgeirsdottir, S. A.; Meijer, D. K.; de Leij, L. F.; Molema, G. Development of vasculature targeting strategies for the treatment of cancer and chronic inflammatory diseases. *Biotechnol. Annu. Rev.* **2002**, *8*, 133–165.
(12) Temming, K.; Schiffelers, R. M.; Molema, G.; Kok, R. J. RGD-based strategies for selective delivery of therapeutics and imaging agents to the tumour vasculature. *Drug Resist. Updates* **2005**, *8*, 381–402.
(13) Sharkey, R. M.; Goldenberg, D. M. Targeted therapy of cancer: New prospects for antibodies and immunoconjugates. *CA Cancer J. Clin.* **2006**, *56*, 226–243.
(14) Austin, C. D.; Wen, X.; Gazzard, L.; Nelson, C.; Scheller, R. H.; Scales, S. J. Oxidizing potential of endosomes and lysosomes limits intracellular cleavage of disulfide-based antibody-drug conjugates. *Proc. Natl. Acad. Sci. U.S.A.* **2005**, *102*, 17987–17992.
(15) Prakash, J.; van Loenen-Weemaes, A. M.; Haas, M.; Proost, J. H.; Meijer, D. K.; Moolenaar, F.; Poelstra, K.; Kok, R. J. Renal-selective delivery and angiotensin-converting enzyme inhibition by subcutaneously administered captopril-lysozyme. *Drug Metab. Dispos.* **2005**, *33*, 683–688.
(16) Burkhart, D. J.; Kalet, B. T.; Coleman, M. P.; Post, G. C.; Koch, T. H. Doxorubicin-formaldehyde conjugates targeting αvβ3 integrin. *Mol. Cancer Ther.* **2004**, *3*, 1593–1604.
(17) Doronina, S. O.; Mendelsohn, B. A.; Bovee, T. D.; Cerveny, C. G.; Alley, S. C.; Meyer, D. L.; Oflazoglu, E.; Toki, B. E.; Sanderson, R. J.; Zabinski, R. F.; Wahl, A. F.; Senter, P. D. Enhanced activity of monomethylauristatin F through monoclonal antibody delivery: Effects of linker technology on efficacy and toxicity. *Bioconjugate Chem.* **2006**, *17*, 114–124.

the cell killing properties in endothelial cells and C26 carcinoma cells.

Experimental Section

Synthesis and Purification of a MMAF–HSA Conjugate. The MMAF–HSA conjugate was prepared as previously described.[3] Briefly, HSA (Sanquin, Amsterdam, The Netherlands) was thiolated with 2-iminothiolane at pH 8 and 37 °C, until an SH/albumin ratio of 4 was reached. The thiol/albumin mole ratio was determined by measuring the thiol concentration with Ellman's assay and the albumin concentration by UV absorbance at 280 nm. The modified albumin was purified over a G25 gel filtration desalting column and treated with a 20% excess (over measured thiols) of the drug linker adduct MC-val-cit-PAB-MMAF. Ellman's assay was performed on the reaction mixture to ensure complete reaction of the thiolated albumin, after which the excess of MC-val-cit-PAB-MMAF was removed with solid-phase resin-bound DTT (BioVectra, Oxford, CO). The final product was purified by size exclusion chromatography (SEC).

Characterization of the MMAF–HSA Conjugate. The concentration of the MMAF–HSA conjugates was measured using the BCA assay kit from Pierce. MMAF–HSA conjugates were analyzed by size exclusion chromatography using a Tosoh Bioscience TSKgel G3000SW (7.8 cm × 30 cm, 5 μm) SEC column and consisted of more than 91% monomer. To check for residual drug linker, a sample of conjugate was treated with MeOH and separated in a microconcentrator to precipitate the protein, after which the supernatant was analyzed by reverse-phase (RP) HPLC [Synergi C12 column with a linear gradient from 5 mM ammonium phosphate (pH 7) to 100% acetonitrile]. No free drug linker was detectable, compared to spiked controls and a standard curve with a quantitation limit of <0.5% of bound drug. The MMAF–HSA conjugates were tested for endotoxin contaminant using a BioWhitaker-Cambrex LAL QCL-1000 kit. Endotoxin was below the limit of detection (<0.05 EU/mg).

The drug to HSA ratio was estimated by treating 300 μg of conjugate with cathepsin B to release free MMAF from the val-cit-PAB linker.[18] The protein was removed by precipitation with a TCA/MeOH mixture, heated at 37 °C for 10 min, and centrifuged at high speed to pellet. The released drug in the supernatant was analyzed by RP-HPLC as described above for the drug linker and quantitated by comparison to a standard curve. The drug/albumin values agreed closely (±5%) with the thiol/albumin ratios determined prior to conjugation. A change in the OD_{250}/OD_{280} ratio commensurating with the conjugation of PAB-containing moieties qualitatively corroborated the measured drug load. Furthemore, the MMAF–HSA conjugate was subjected to MALDI-TOF analysis as described previously to calculate the number of attached MMAF molecules per HSA.[19] To this end, HSA and MMAE–HSA were dissolved in a 50/50/0.1 methanol/water/acetic acid mixture at a concentration of 1 mg/mL. One microliter was mixed with 1 μL of matrix (20 mg/mL sinapinic acid in a 60/40/0.1 water/acetonitrile/trifluoroacetic acid mixture), transferred onto a stainless steel sample holder, and dried before being introduced into a Voyager-DE PRO workstation (Applied Biosystems). Mass spectra were obtained by averaging the signals from 100 laser shots. Correction of data was performed using BSA as a control.

Synthesis of RGDPEG–MMAF–HSA. RGDPEG–MMAF–HSA was synthesized as described previously for RGDPEG–MMAE–HSA.[3] In short, MMAF–HSA was incubated with a 50-fold molar excess of vinylsulfone-polyethyleneglycol-*N*-hydroxysuccinimide ester (VNS-PEG-NHS; Nektar; 30 mg/mL in water, 1.48 μmol) in PBS. After incubation for 1 h, RGD-peptide c[RGDf(ε-*S*-acetylthioacetyl)K] (Ansynth Service, Roosendaal, The Netherlands) dissolved at 10 mM in a 1/4 acetonitrile/water mixture and was added to the reaction mixture at a peptide to protein molar ratio of 55/1, after which hydroxylamine was added to a final concentration of 50 mM. Reaction was carried out overnight at room temperature, and remaining VNS groups were quenched by addition of cysteine for 1 h at room temperature (55-fold molar excess over the amount of HSA). Thereafter, the product was dialyzed three times against PBS at 4 °C using Slide-A-Lyzer dialysis cassettes (Pierce, molecular mass cutoff of 10 kDa) and finally purified by SEC using a Superdex200 column on an Äkta system (GE Healthcare, Uppsala, Sweden) with PBS as the mobile phase. The final product RGDPEG–MMAF–HSA was stored at −20 °C. A control RADPEG–MMAF–HSA conjugate was prepared according to the same protocol with the control peptide c[RADf(ε-*S*-acetylthioacetyl)K].

Synthesis of RGD–MMAF–HSA. RGD–MMAF–HSA was synthesized as described previously for RGD–MMAE–HSA.[3] In short, MMAF–HSA was incubated with a 22-fold molar excess of iodoacetic acid *N*-hydroxysuccinimide ester (SIA linker; Sigma, St. Louis, MO). RGD-peptide was added in a mole/mole ratio of 25/1 followed by addition of hydroxylamine as described above. Reaction was carried out within 6 h at room temperature while the mixture was protected from light. Products were purified by dialysis against PBS. The final product RGD–MMAF–HSA and the control conjugate RAD–MMAF–HSA were stored at −20 °C.

Characterization of RGDPEG–MMAF–HSA and RGD–MMAF–HSA Conjugates. The protein content of synthesis products was estimated with a BCA protein assay

(18) Sanderson, R. J.; Hering, M. A.; James, S. F.; Sun, M. M.; Doronina, S. O.; Siadak, A. W.; Senter, P. D.; Wahl, A. F. In vivo drug-linker stability of an anti-CD30 dipeptide-linked auristatin immunoconjugate. *Clin. Cancer Res.* **2005**, *11*, 843–852.

(19) Temming, K.; Lacombe, M.; van der Hoeven, P.; Prakash, J.; Gonzalo, T.; Dijkers, E. C. F.; Orfi, L.; Keri, G.; Poelstra, K.; Molema, G.; Kok, R. J. Delivery of the p38 MAPkinase inhibitor SB202190 to angiogenic endothelial cells: Development of novel RGD-equipped and pegylated drug-albumin conjugates using platinum(II) based drug linker technology. *Bioconjugate Chem.* **2006**, *17*, 1246–1255.

kit (Pierce). Both the intermediate and final products were subjected to analytical SEC to reveal increases in size, purity, and grade of aggregation. The Äkta system (GE Healthcare) was equipped with a Superdex200 column, and PBS was used as the mobile phase. We also used SEC to estimate hydrodynamic size in comparison to a range of differently sized proteins: cytochrome *c* (12.4 kDa), carbonic anhydrase (29 kDa), HSA (66.4 kDa), alcohol dehydrogenase (150 kDa), amylase (200 kDa), ferritin (440 kDa), thyroglobulin (669 kDa), and Gel Filtration Molecular Weight Marker (Sigma). RGD peptide incorporation was corroborated using an in-house-prepared rabbit anti-RGD antiserum.[20] To this end, drug targeting conjugates and the control RGD–HSA were placed on a nitrocellulose membrane (Bio-Rad, Hercules, CA) and dried. The membrane was blocked with BSA (1% in PBS) for 1 h, washed, and subsequently incubated with an in-house-raised rabbit anti-RGD antiserum for 1 h at room temperature. After another washing step, the signal was amplified with a polyclonal goat anti-rabbit IgG conjugated with horseradish peroxidase (GARPO, DAKO). Peroxidase was visualized by incubation with 3-amino-9-ethylcarbazole (AEC, Sigma). The amount of RGDPEG and RGD bound per HSA was determined by MALDI-TOF analysis as explained above.

Cells. HUVEC were obtained from the UMCG Endothelial Cell Facility. Primary isolates were cultured in 1% gelatin-coated tissue culture flasks (Costar, Cambridge, MA) at 37 °C under a 5% CO_2/95% air atmosphere. The culture medium, hereafter termed EC medium, consisted of RPMI 1640 (BioWittaker, Verviers, Belgium) supplemented with 20% heat-inactivated fetal calf serum (Integro, Zaandam, The Netherlands), 2 mM L-glutamine (Invitrogen, Breda, The Netherlands), 5 units/mL heparin (Leo Pharmaceutical Products, Weesp, The Netherlands), 100 units/mL penicillin (Yamanouchi Pharma, Leiderdorp, The Netherlands), 100 μg/mL streptomycin (Radiumfarma-Fisiopharma), and 50 μg/mL EC growth factor supplement extracted from bovine brain. After attaining confluence, cells were detached from the surface by trypsin EDTA (0.5/0.2 mg/mL in PBS) treatment and split in a 1/3 ratio. Cells were used up to passage 4.

C26 mouse carcinoma cells were cultured in DMEM (Gibco) containing 2 mM L-glutamine (Invitrogen), 100 units/mL penicillin (Yamanouchi Pharma), 100 μg/mL streptomycin (Radiumfarma-Fisiopharma), and 10% heat-inactivated fetal calf serum. After attaining confluence, cells were detached from the surface by trypsin EDTA (0.5/0.2 mg/mL in PBS) treatment and split in a 1/10 ratio.

In Vitro Killing Efficacy of Auristatin-Equipped Conjugates. HUVEC or C26 carcinoma cells were plated on 96-well plates (Costar) at a density of 5000 cells/well for HUVEC and 10000 cells/well for C26 cells and exposed to a graded titration of drug targeting conjugates. RAD-equipped control conjugates were tested at concentrations of 0.1, 1, and 10 μg/mL. After incubation for 72 h, cell viability was determined with a MTS cell viability assay (Promega, Madison, WI).[21] Absorption was measured on a Thermomax microplate reader (Molecular Devices, Sunnyvale, CA) at 490 nm after incubation for 2 h (HUVEC) or 40 min (C26 cells) at 37 °C. All results are based on triplicate samples, and experiments were repeated at least three times. Data were analyzed by nonlinear regression using GraphPad Prism (GraphPad Software Inc.). All EC_{50} values were calculated using a fixed bottom (10% viability) and a fixed top (100% viability).

Statistical Analysis. Statistical analysis was performed using a Student's two-tailed *t* test, assuming equal variances.

Results and Discussion

Monomethyl auristatin E and F are potent derivatives of the natural product dolostatin 10 that inhibits tubulin polymerization in dividing cells and thereby induces apoptosis.[22,23] Monomethyl auristatin F is a new auristatin derivative with impaired membrane translocation capabilities due to a C-terminal domain that is charged at physiological pH (Figure 1). Previous studies have shown that the activity of MMAF is greatly potentiated through active delivery via an antibody–drug conjugate (ADC), suggesting that MMAF as a free drug is not able to easily cross cellular membranes.[17] Similarly, the noncharged *O*-methyl prodrug of MMAF proved to be very cytotoxic in cell-based assays, displaying activity up to 5 orders of magnitude higher (EC_{50} = 0.001–0.1 nM). Once ADCs containing MMAF are internalized and hydrolyzed within lysosomes, free drug is rapidly released from the self-immolative linker. Lysosomal uptake of MMAF–Ab conjugates, drug release, and subsequent effects have been demonstrated, indicating that MMAF does reach the cytosol after intracellular delivery.[24,25] Although one may speculate that transport of MMAF from the lysosomal compartment to the cytosol is mediated by passive diffusion, the expected pK_a of the phenylalanine group (ca. 2.6) will provide only a small noncharged fraction at

(20) Kok, R. J.; Schraa, A. J.; Bos, E. J.; Moorlag, H. E.; Asgeirsdottir, S. A.; Everts, M.; Meijer, D. K.; Molema, G. Preparation and functional evaluation of RGD-modified proteins as $\alpha_v\beta_3$ integrin directed therapeutics. *Bioconjugate Chem.* **2002**, *13*, 128–135.

(21) Alley, M. C.; Scudiero, D. A.; Monks, A.; Hursey, M. L.; Czerwinski, M. J.; Fine, D. L.; Abbott, B. J.; Mayo, J. G.; Shoemaker, R. H.; Boyd, M. R. Feasibility of drug screening with panels of human tumor cell lines using a microculture tetrazolium assay. *Cancer Res.* **1988**, *48*, 589–601.

(22) Pettit, G. R. The dolastatins. *Fortschr. Chem. Org. Naturst.* **1997**, *70*, 1–79.

(23) Doronina, S. O.; Toki, B. E.; Torgov, M. Y.; Mendelsohn, B. A.; Cerveny, C. G.; Chace, D. F.; DeBlanc, R. L.; Gearing, R. P.; Bovee, T. D.; Siegall, C. B.; Francisco, J. A.; Wahl, A. F.; Meyer, D. L.; Senter, P. D. Development of potent monoclonal antibody auristatin conjugates for cancer therapy. *Nat. Biotechnol.* **2003**, *21*, 778–784.

(24) Sutherland, M. S.; Sanderson, R. J.; Gordon, K. A.; Andreyka, J.; Cerveny, C. G.; Yu, C.; Lewis, T. S.; Meyer, D. L.; Zabinski, R. F.; Doronina, S. O.; Senter, P. D.; Law, C. L.; Wahl, A. F. Lysosomal trafficking and cysteine protease metabolism confer target-specific cytotoxicity by peptide-linked anti-CD30-auristatin conjugates. *J. Biol. Chem.* **2006**, *281*, 10540–10547.

Scheme 1. Synthesis of Drug Targeting Conjugates

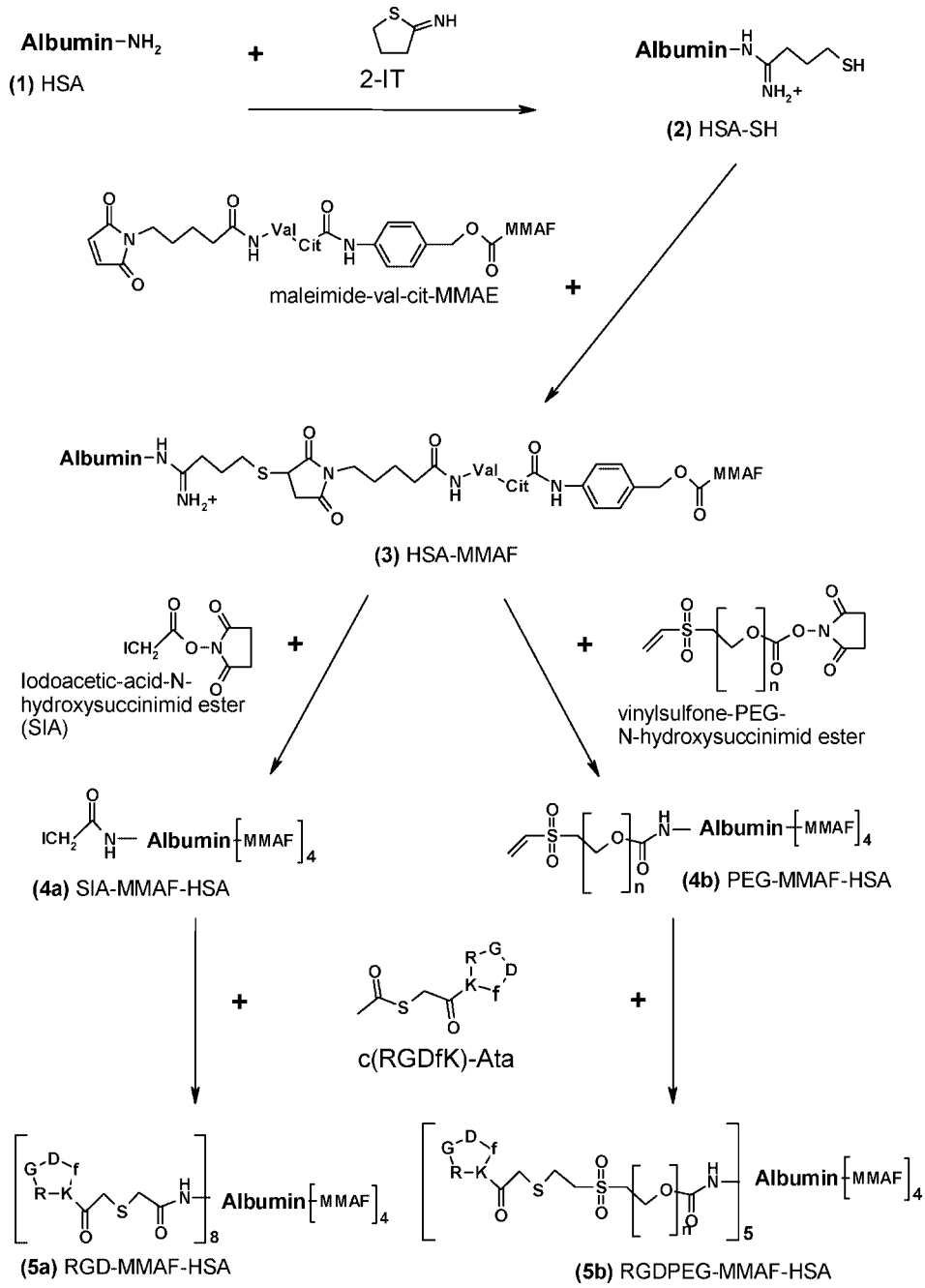

lysosomal pH (i.e., 0.1% of the total lysosomally present drug at pH 5.5). Alternatively, transport of peptidic or charged compounds across the lysosomal membrane may be receptor-mediated as reviewed by Lloyd.[26] In contrast to MMAF, MMAE is more lipophilic and does not contain the charged phenylalanine residue. Hence, the compound will cross cell membranes more easily, which can also be deduced by the difference in the EC_{50} values of the free drugs (0.1–2.0 nM for MMAE and 100–250 nM for MMAF).[17] Prior studies with MMAF–antibody conjugates showed a higher potency as compared to the corresponding MMAE immunoconjugates,[17,27,24] which is in agreement with the difference in cellular retention. In the current study, we developed RGD–MMAF–albumin conjugates for the targeted, intracel-

(25) Polson, A. G.; Yu, S. F.; Elkins, K.; Zheng, B.; Clark, S.; Ingle, G. S.; Slaga, D. S.; Giere, L.; Du, C.; Tan, C.; Hongo, J. A.; Gogineni, A.; Cole, M. J.; Vandlen, R.; Stephan, J. P.; Young, J.; Chang, W.; Scales, S. J.; Ross, S.; Eaton, D.; Ebens, A. Antibody-drug conjugates targeted to CD79 for the treatment of non-Hodgkin's lymphoma. *Blood,* in press.

(26) Lloyd, J. B. Lysosome membrane permeability: Implications for drug delivery. *Adv. Drug Delivery Rev.* **2000**, *41*, 189–200.

(27) Jeffrey, S. C.; Andreyka, J. B.; Bernhardt, S. X.; Kissler, K. M.; Kline, T.; Lenox, J. S.; Moser, R. F.; Nguyen, M. T.; Okeley, N. M.; Stone, I. J.; Zhang, X.; Senter, P. D. Development and properties of β-glucuronide linkers for monoclonal antibody-drug conjugates. *Bioconjugate Chem.* **2006**, *17*, 831–840.

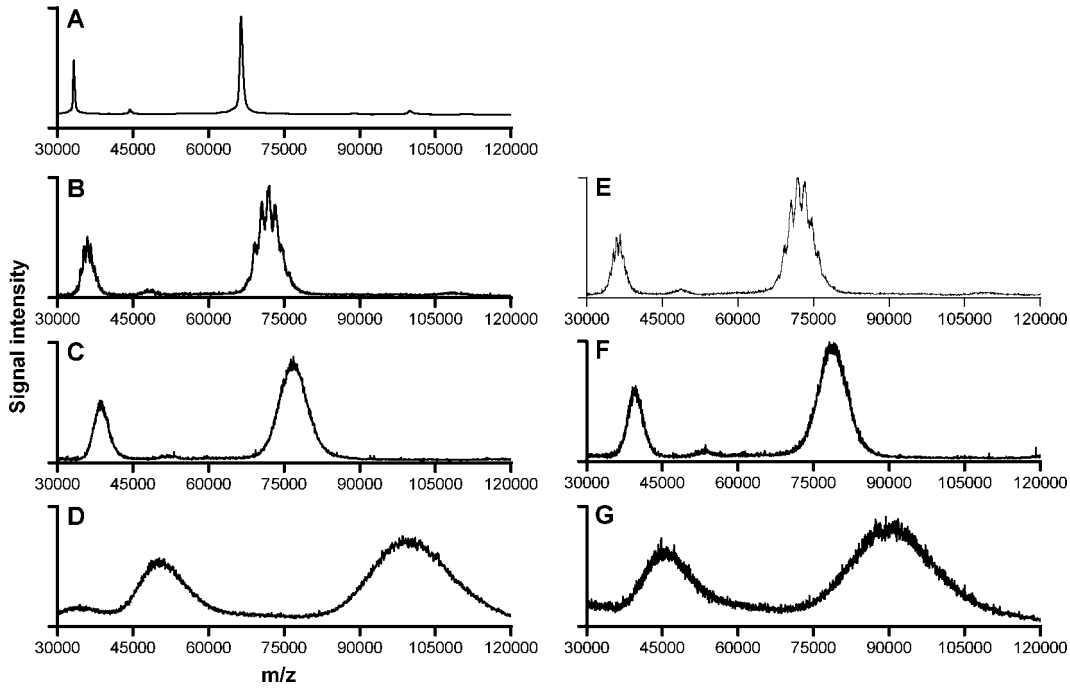

Figure 2. Molecular weight of drug targeting conjugates. MALDI-TOF analysis of HSA (A), MMAF–HSA (B), RGD–MMAF–HSA (C), RGDPEG–MMAF–HSA (D), MMAF–HSA (E), RGD–MMAE–HSA (F), and RGDPEG–MMAE–HSA (G) revealed an increase in size due to modification of the albumin carrier.

Table 1. Modifications of Albumin As Determined by MALDI-TOF

conjugate	MMAF/HSA coupling ratio (mol/mol)	RGD(PEG)/HSA coupling ratio (mol/mol)	molecular mass (kDa)
RGD–MMAF–HSA	4.2	7.2	77.1
RGDPEG–MMAF–HSA	4.2	6.8	100
RGD–MMAE–HSA	4.1	7.6	77.3
RGDPEG–MMAE–HSA	4.1	5.4	94.5

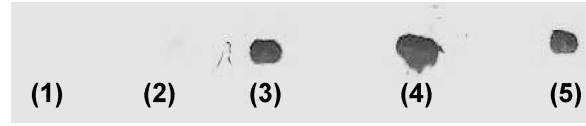

Figure 3. Conjugation of RGD-peptide. Anti-RGD dot blot was performed to corroborate conjugation of RGD to albumin. HSA (1) and MMAF–HSA (2) were not recognized by the anti-RGD antibody, while RGD–MMAF–HSA (3), RGDPEG–MMAF–HSA (4), and RGD–HSA (5) were positively stained for RGD.

lular delivery of the drug into tumor endothelial cells. MMAF was coupled to the albumin backbone using a lysosomally cleavable valine–citrulline linker (Scheme 1). HPLC analysis of released drug demonstrated an average of four MMAF molecules per albumin (Table 1), which is identical to the number of MMAE molecules per albumin, as described previously by us.[3] Furthermore, most reported auristatin–antibody conjugates also contain four drugs per antibody.[28] RP-HPLC showed that the products did not contain free drug or linker molecules (below the limit of quantitation; <0.5% of the bound drug), while MALDI-TOF analysis corroborated the number of auristatin molecules bound per albumin (Table 1 and Figure 2).

It has been recognized that RGD-based drug targeting conjugates need to be equipped with multiple RGD-peptides to achieve optimal binding and uptake into the targeted cell.[12,29,30] MALDI-TOF analysis allowed the determination of the number of RGD peptides that were coupled via a short SIA or extended PEG linker (Table 1 and Figure 2). Again, these numbers closely corresponded to the average RGD/albumin ratios found for MMAE–albumin conjugates. Furthermore, we confirmed coupling of RGD-peptide onto the distal end of PEG by anti-RGD dot blot. Both products as well as the control RGD–HSA were positively stained with anti-RGD antibody, while MMAF–HSA and HSA were devoid of staining (Figure 3).

Apart from MALDI-TOF, we used analytical size exclusion chromatography to study the size and purity of our drug

(28) Hamblett, K. J.; Senter, P. D.; Chace, D. F.; Sun, M. M.; Lenox, J.; Cerveny, C. G.; Kissler, K. M.; Bernhardt, S. X.; Kopcha, A. K.; Zabinski, R. F.; Meyer, D. L.; Francisco, J. A. Effects of drug loading on the antitumor activity of a monoclonal antibody drug conjugate. *Clin. Cancer Res.* **2004**, *10*, 7063–7070.

(29) Schraa, A. J.; Kok, R. J.; Berendsen, A. D.; Moorlag, H. E.; Bos, E. J.; Meijer, D. K.; de Leij, L. F.; Molema, G. Endothelial cells internalize and degrade RGD-modified proteins developed for tumor vasculature targeting. *J. Controlled Release* **2002**, *83*, 241–251.

(30) Wester, H. J.; Kessler, H. Molecular targeting with peptides or peptide-polymer conjugates: Just a question of size? *J. Nucl. Med.* **2005**, *46*, 1940–1945.

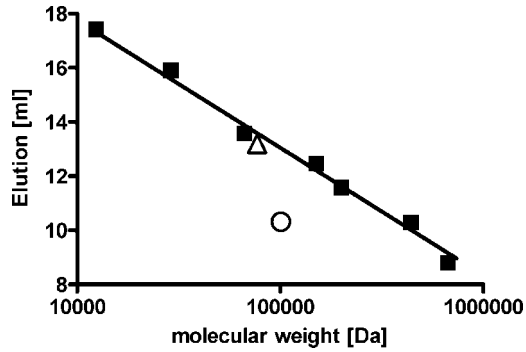

Figure 4. Hydrodynamic volume of drug targeting conjugates. Elution volumes in SEC of a range of proteins (■) were plotted against their molecular weight. Elution volumes of RGD–MMAF–HSA (△) and RGDPEG–MMAF–HSA (○) were plotted against the molecular weight as detected by MALDI-TOF. It can be seen that elution volumes closely correlated with the molecular weight ($R = 0.99$) except for that of the PEG-containing conjugate which displayed an aberrant elution volume.

targeting conjugates. SEC revealed only 3% of aggregates in the products, mainly dimeric HSA, which is comparable to the extent of aggregation found for the parental HSA used in our studies (data not shown). The elution volumes of the drug targeting conjugates were compared to a range of different sized globular proteins. Figure 4 shows that the elution volume of RGD–MMAF–HSA closely correlated with the standard curve of globular proteins. In contrast, RGDPEG–MMAF–HSA eluted at an elution volume typical for a 370 kDa protein, although its actual size as determined by MALDI-TOF was only 100 kDa. The observed apparent size of the macromolecule was introduced by the 3.5 kDa PEG linker that is used for RGD coupling and nicely illustrates the extended conformation of the PEG–RGD arm. Likely, the incorporation of PEG into the targeted construct further improves tumor targeting by the enhanced permeability and retention (EPR) effect.[31] Taken together, the synthesis approaches for both types of conjugates with either PEG or SIA linker groups led to well-characterized products with little aggregation and no detectable impurities.

Earlier, we showed that RGD-modified albumin conjugates bind with high avidity to $\alpha_v\beta_3$-integrin-expressing cells and are subsequently internalized.[19,3,4] Since the RGD/albumin ratios of the conjugates developed here were comparable to those of previously developed RGD–albumin conjugates, we expected similar binding and uptake characteristics for the new conjugates. We furthermore demonstrated binding and uptake by both endothelial cells (HUVEC) and C26 tumor cells that express $\alpha_v\beta_3$-integrin. Although the approach of $\alpha_v\beta_3$-targeted auristatins using RGD-peptides generally aims at angiogenic endothelium in solid tumors, it can also have

(31) Tanaka, T.; Shiramoto, S.; Miyashita, M.; Fujishima, Y.; Kaneo, Y. Tumor targeting based on the effect of enhanced permeability and retention (EPR) and the mechanism of receptor-mediated endocytosis (RME). *Int. J. Pharm.* **2004**, *277*, 39–61.

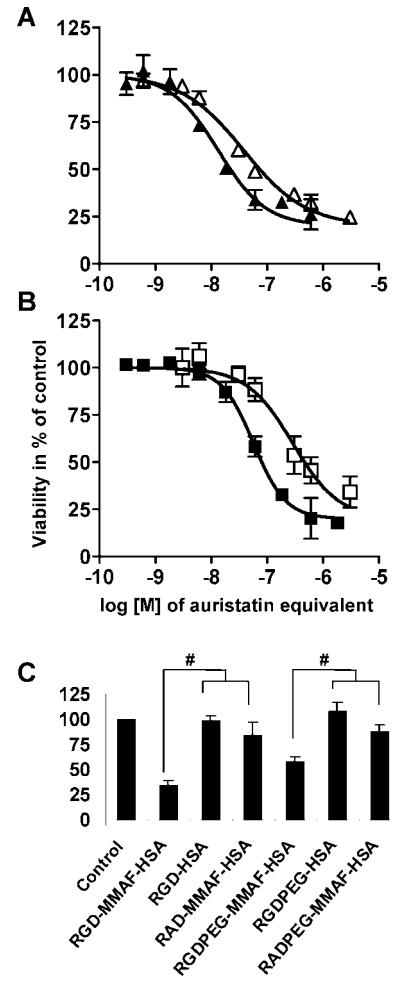

Figure 5. Effect of drug targeting conjugates on endothelial cell viability. HUVEC have been incubated with increasing concentrations of drug targeting conjugates to determine killing efficacy. Molar concentrations of drug targeting conjugates are expressed as conjugated drug equivalent in panels A and B. (A) Effect of RGD–MMAF–HSA (▲) on the viability of HUVEC compared with the effect of RGD–MMAE–HSA (△). (B) Effect of RGDPEG–MMAF–HSA (■) on the viability of HUVEC compared with the effect of RGDPEG–MMAE–HSA (□). It can be appreciated from panels A and B that MMAF conjugates display only a modest improvement in potency over MMAE conjugates when tested on endothelial cells. (C) Viability of cells treated with either 1 μg/mL drug targeting conjugate or different control conjugates. Differences between drug targeting conjugates and the respective control conjugates were statistically significant with a p of <0.01. Data for MMAE drug targeting conjugates were taken from ref 3.

the tumor cells as a secondary target. Many tumor types are known to express $\alpha_v\beta_3$-integrin, and the expression levels correlate well with tumor progression in malignancies, like, for example, breast cancer,[32] glioma,[33] and melanoma.[34] We previously demonstrated such dual targeting for C26 colon carcinoma cells since RGD-targeted MMAE bound to HUVEC and C26 cells.[3]

Table 2. Cell Killing Properties of Drug Targeting Conjugates[a]

	EC_{50} tested on HUVEC		EC_{50} tested on C26 tumor cells	
compound	in nM drug equiv	95% CI[b]	in nM drug equiv	95% CI[b]
RGD–MMAF–HSA	22	11.5–42	8.7	6.7–11.2
RGDPEG–MMAF–HSA	77	62–95	147	123–175
RGD–MMAE–HSA	65	38–112	533	310–915
RGDPEG–MMAE–HSA	420	225–780	2070	1580–2710

[a] Results are based on triplicate samples, and experiments were performed at least three times. [b] CI, confidence interval.

We studied the effect of intracellularly delivered MMAF on viability of HUVEC and found that RGD–MMAF–HSA and RGDPEG–MMAF–HSA efficiently killed HUVEC with EC_{50} values of 20–80 nM conjugated drug equivalent (Figure 5 and Table 2). Control conjugates with nontargeted RAD peptide or without MMAF modification did not influence cell viability at this concentration (Figure 5C). Drug targeting conjugates in which the RGD-peptide was introduced by using a short alkyl linker were 3.5–16-fold more cytotoxic than conjugates in which a PEG linker was used. In part, this can be attributed to the higher RGD/carrier ratio, gained by application of the short alkyl linker, which leads to a higher binding affinity. Furthermore, the different spatial presentation of RGD-peptides coupled by different linkers or the difference in hydrophobicity between the linkers might have an influence on binding affinity, uptake, and in vitro efficacy. Whether the reduced in vitro efficacy of PEG-containing drug targeting conjugates is offset by prolonged circulation times and improved passive retention remains to be shown in vivo.

In comparison to the previously reported MMAE–albumin conjugates, the new MMAF–HSA conjugates exhibited a 3–6-fold increase in potency when tested on HUVEC. Similar observations have been made for the MMAE- and MMAF-modified antibodies c1F6 and cAC10 against CD70 and CD30, respectively.[17,27,24] MMAF-modified antibodies proved to be 1.2–6-fold more potent in killing of tumor cell lines than the respective MMAE antibodies. We now tested MMAE– and MMAF–albumin conjugates on C26 carcinoma cells, and targeted MMAF was found also to kill this cell type effectively with EC_{50} values of 9–150 nM for the coupled drug equivalent (Figure 6 and Table 2). In contrast, MMAE conjugates were somewhat less potent with EC_{50} values which were between 14- and 62-fold lower than that of the respective MMAF conjugate. If we furthermore take the EC_{50} values of free MMAE (0.1–2.0 nM)[17] and free MMAF (100–250 nM)[17] into account, we see that free

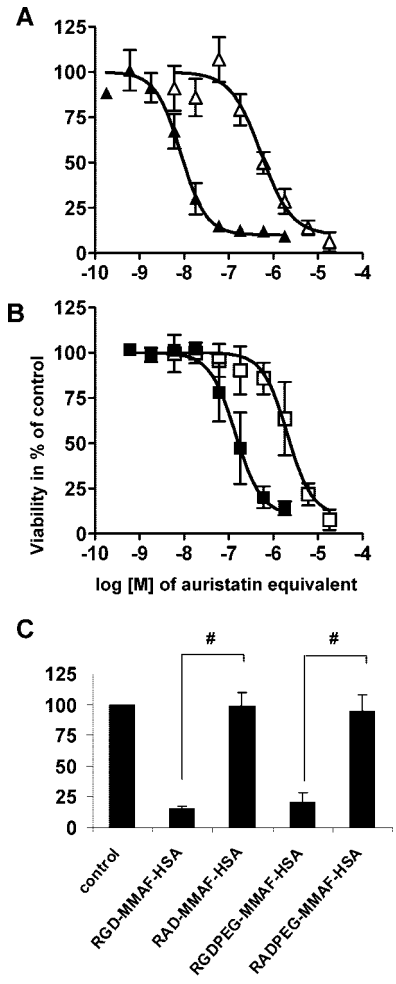

Figure 6. Effect of drug targeting conjugates on tumor cell viability. C26 colon carcinoma cells have been incubated with increasing concentrations of drug targeting conjugates to determine killing efficacy. Molar concentrations of drug targeting conjugates are expressed as conjugated drug equivalent in panels A and B. (A) Effect of RGD–MMAF–HSA (▲) on C26 viability compared with the effect of RGD–MMAE–HSA (△). (B) Effect of RGDPEG–MMAF–HSA (■) on C26 viability compared with the effect of RGDPEG–MMAE–HSA (□). Notice that MMAF conjugates displayed a considerable improvement in potency over MMAE conjugates when tested on C26 cells. (C) Viability of cells treated with either 1 μg/mL RGD–MMAF–HSA or the control RAD–MMAF–HSA or with 10 μg/mL RGDPEG–MMAF–HSA or the control RADPEG–MMAF–HSA. Differences between drug targeting conjugates and respective control conjugates were significant with a p of <0.001.

(32) Chen, X.; Park, R.; Tohme, M.; Shahinian, A. H.; Bading, J. R.; Conti, P. S. MicroPET and autoradiographic imaging of breast cancer αv-integrin expression using ^{18}F- and ^{64}Cu-labeled RGD peptide. *Bioconjugate Chem.* **2004**, *15*, 41–49.

(33) Chen, X.; Park, R.; Hou, Y.; Khankaldyyan, V.; Gonzales-Gomez, I.; Tohme, M.; Bading, J. R.; Laug, W. E.; Conti, P. S. MicroPET imaging of brain tumor angiogenesis with ^{18}F-labeled PEGylated RGD peptide. *Eur. J. Nucl. Med. Mol. Imaging* **2004**, *31*, 1081–1089.

(34) Schmieder, A. H.; Winter, P. M.; Caruthers, S. D.; Harris, T. D.; Williams, T. A.; Allen, J. S.; Lacy, E. K.; Zhang, H.; Scott, M. J.; Hu, G.; Robertson, J. D.; Wickline, S. A.; Lanza, G. M. Molecular MR imaging of melanoma angiogenesis with $\alpha_v\beta_3$-targeted paramagnetic nanoparticles. *Magn. Reson. Med.* **2005**, *53*, 621–627.

MMAE is more cytotoxic than the respective MMAE–albumin conjugates but free MMAF is much less toxic than the respective RGD-equipped MMAF–albumin conjugates. Similar observations have been made for antibody-based drug–carrier conjugates.[24,17] Thus, intracellular delivery by means of a receptor-mediated internalization process turned MMAF into a highly potent cytotoxic agent. In another approach, a methylated species of MMAF (MMAF-OMe) was studied. The esterification of the carboxyl group and, hence, the removal of the charged group of MMAF turned the product into a very potent compound ($EC_{50} = 0.001–0.01$ nM) which was much more cytotoxic than MMAE.[17] Since the *O*-methylester can be converted into the MMAF parent by cytosolic esterases, a plausible explanation is that MMAF-OMe is converted intracellularly into MMAF, which will be retained intracellularly due to its charged nature. In conclusion, the differences in cell killing efficacy of targeted MMAE and MMAF are likely due to a combination of the relative potencies of the respective drugs, together with the enhanced retention of MMAF within the tumor cells due to the negative charge present on the C-terminal phenylalanine residue. When challenged to speculate about the relative importance of the two factors (intrinsic potency or cellular retention), we believe that the second factor is most important. This assumption is supported by the studies with MMAF mentioned above. It is very plausible that MMAF is unable to enter cells due to its charged state at neutral pH, and masking of this charge (in MMAF-OMe) improved the EC_{50} 100000-fold. Thus, it is also plausible that the compound is efficiently retained subsequent to its intracellular delivery. The accumulation of compound within the cells will by far compensate for the differences in intrinsic activity, especially when prolonged uptake can be ensured, for instance, by ensuring that the receptor-mediated uptake is taking place efficiently.

Our results demonstrate that RGD–auristatin–HSA conjugates exert potent activities on $\alpha_v\beta_3$-positive endothelial and colorectal carcinoma cells. These conjugates would be expected to exert in vivo antitumor activity through the direct elimination of both tumor cells and the vascular endothelium that feed them. The drugs used in these studies may be ideally suited for these particular activities, since a structurally related agent, TZT-1027, has also been shown to exert potent activities on tumor vasculature.[35] The fact that the MMAF conjugates are more potent than the MMAE counterparts is not surprising, given that MMAF is one of the most potent auristatins yet described,[17] and it may have enhanced retention inside cells upon drug release. The data reported here support further evaluation of both molecular classes, which would include in vivo efficacy and toxicological studies.

Acknowledgment. We thank H. E. Moorlag from the UMCG Endothelial Cell Facility for skillful isolation and culturing of HUVEC. A. J. Lexmond and R. Habich are acknowledged for their support during synthesis and in vitro evaluation. This work was made possible by grants from Marie Curie (HPMI-CT-2002-00218) and SenterNovem (TSGE1083).

MP0700312

(35) Otani, M.; Natsume, T.; Watanabe, J. I.; Kobayashi, M.; Murakoshi, M.; Mikami, T.; Nakayama, T. TZT-1027, an antimicrotubule agent, attacks tumor vasculature and induces tumor cell death. *Jpn. J. Cancer Res.* **2000**, *91*, 837–844.